

# Microstructure and squareness factor: A quantitative correlation in (Nd, Pr)FeB sintered magnets

E. A. Périgo,<sup>a)</sup> H. Takiishi, C. C. Motta, and R. N. Faria

*Instituto de Pesquisas Energéticas e Nucleares (IPEN)-CNEN, São Paulo 05508-900, Brazil  
and Centro Tecnológico da Marinha em São Paulo (CTMSP), São Paulo 05508-900, Brazil*

(Received 30 July 2007; accepted 17 October 2007; published online 10 December 2007)

A quantitative correlation between the microstructure and squareness factor of  $R_{16}\text{Fe}_{76}\text{B}_8$  ( $R=\text{Nd}$  or  $\text{Pr}$ ) sintered magnets is proposed. The expression was derived based on the micrographs of 19 magnets, making a total of more than 11 000 grains analyzed. This expression is independent of the determination of the sample's magnetic properties. Magnet processing conditions were used to modify the microstructure and, hence, the squareness factor. Six microstructural parameters—grain size, grain elongation, grain roundness, and their respective standard deviations—were quantified using an image analyzer software program. The squareness factor was higher for magnets with a microstructure showing rounder grains and a sharp size distribution. A comparison of the squareness factor obtained by the proposed expression with that calculated from the demagnetization curve showed a fairly good agreement. Some disparities were also found and are discussed herein. © 2007 American Institute of Physics. [DOI: 10.1063/1.2821756]

## I. INTRODUCTION

A permanent magnet with a high squareness factor (SF), preferentially equal to unity, is desired in order to guarantee the magnetic stability.<sup>1</sup> The mean grain size is normally used to associate the magnetic properties and microstructure of RFeB compounds.<sup>2–9</sup> However, the grain size distribution, grain shape, grain surface inhomogeneities, intergrain region, volume of additional phases, and their spatial distribution also play an important role in the profile of the demagnetization curve.<sup>10–13</sup> No systematic studies correlating SF and microstructural parameters have been reported in the literature so far. In this study, a quantitative correlation between the microstructure and the SF of  $R_{16}\text{Fe}_{76}\text{B}_8$  sintered magnets is proposed. Both the size and shape of the  $R_2\text{Fe}_{14}\text{B}$  phase grains were evaluated.

## II. EXPERIMENTAL

$R_{16}\text{Fe}_{76}\text{B}_8$  sintered magnets were used in this investigation. Details of the samples' preparation and identification are summarized in Table I. The squareness factor was obtained by two distinct routes. The first route is from the second quadrant of the  $M \times H$  curve, defined by

$$\text{SF} = \frac{\mu_0 H_k}{\mu_{0i} H_c}, \quad (1)$$

where  $\mu_0 H_k$  refers to the reverse field at 90% of  $B_r$ .<sup>2,14</sup> The second route is from polished and chemically etched surfaces parallel to the magnetization vector direction, visualized under a scanning electron microscope. At least 600 grains were analyzed for each sample. Using an image analyzer software program, the following microstructural parameters were quantified:

- Grain size: the diameter of a circle with the same area as the two-dimensional image of the original grain.<sup>15</sup>
- Grain elongation: the ratio of the length of the minor axis to the length of the major axis of a grain, where the latter maintains a perpendicularity with the major axis.<sup>16</sup> In this work, the inverse relationship was used.
- Grain roundness: the ratio of the area of a grain multiplied by  $4\pi$  to its square perimeter.<sup>16</sup>

Mean grain size ( $\bar{\chi}_{\text{GS}}$ ), elongation ( $\bar{\chi}_E$ ), and roundness ( $\bar{\chi}_R$ ) and their respective standard deviations ( $\sigma_{\text{GS}}$ ,  $\sigma_E$ , and  $\sigma_R$ ) were calculated for all the quantities described. Based on these microstructural parameters, as shown in Fig. 1, the homogeneity of RFeB sintered magnets was estimated and divided into two categories: (i) size homogeneity, represented by the mean grain size and its standard deviation, and (ii) shape homogeneity, represented by the grain roundness and elongation, with their respective standard deviations. The section below contains a quantitative discussion about this methodology.

## III. RESULTS AND DISCUSSION

The microstructure and SF were initially correlated for  $\text{Pr}_{16}\text{Fe}_{76}\text{B}_8$  magnets fast cooled after sintering and annealing (samples 1–3 in Table I). Increasing the annealing time caused both the mean grain size of  $\text{Pr}_2\text{Fe}_{14}\text{B}$  and its respective standard deviation to become larger. Annealing controls size homogeneity and its increase is detrimental to the SF. After 35 h,  $\sigma_{\text{GS}}$  represented about 81% of  $\bar{\chi}_{\text{GS}}$ . Statistically, grains with dimensions between 1.6 and 15.5  $\mu\text{m}$  can be found. On the other hand, annealing is a beneficial process to improve the shape homogeneity of  $\text{Pr}_2\text{Fe}_{14}\text{B}$  grains. Mean grain elongation  $\bar{\chi}_E$  decreased by around 7% between 2 and 35 h of annealing, and  $\sigma_E$  dropped by about 23%. Nevertheless, the mean grain roundness  $\bar{\chi}_R$  and its standard deviation

<sup>a)</sup>Electronic mail: eaperigo@ieec.org.

TABLE I. Sample identification, details of preparation, microstructural parameters, and squareness factors of sintered  $R_{16}Fe_{76}B_8$  magnets. P16= $Pr_{16}Fe_{76}B_8$ ; N16= $Nd_{16}Fe_{76}B_8$ ; RBM=roller ball milling; PBM=planetary ball milling, I=isotropic.

Sample ID	Composition/HD time	Milling	Cooling	Annealing	$\bar{X}_{GS} \pm \sigma_{GS}$ ( $\mu m$ )	$\bar{X}_E \pm \sigma_E$ ( $\mu m$ )	$\bar{X}_R \pm \sigma_R$ ( $\mu m$ )	SF (no unit)	sf (no unit)	Ref.
1	P16—1 h	RBM, 20 h	Fast	1000 °C—2 h	5.44±2.62	1.54±0.44	0.81±0.10	0.82	0.80	This work
2	P16—1 h	RBM, 20 h	Fast	1000 °C—15 h	6.03±3.40	1.51±0.41	0.81±0.09	0.76	0.78	This work
3	P16—1 h	RBM, 20 h	Fast	1000 °C—35 h	8.55±6.92	1.43±0.34	0.83±0.08	0.76	0.73	This work
4	P16—1 h	RBM, 18 h	Slow	No	5.67±2.24	1.50±0.36	0.56±0.10	0.77	0.84	This work
5	P16—1 h	RBM, 27 h	Slow	No	4.29±1.71	1.47±0.32	0.61±0.11	0.79	0.84	This work
6	P16—1 h	RBM, 45 h	Slow	No	4.20±1.64	1.53±0.41	0.66±0.09	0.84	0.84	This work
7	N16—1 h	RBM, 18 h	Slow	No	3.70±1.41	1.60±0.44	0.53±0.09	0.82	0.83	This work
8	N16—1 h	RBM, 45 h	Slow	No	5.38±2.11	1.49±0.39	0.56±0.09	0.85	0.83	This work
9	P16—1 h	PBM, 0.50 h	Slow	No	4.96±2.78	1.80±0.80	0.60±0.16	0.54	0.55	17
10	P16—1 h	PBM, 0.75 h	Slow	No	4.21±2.80	1.62±0.50	0.66±0.13	0.65	0.66	17
11	P16—1 h	PBM, 1.00 h	Slow	No	3.51±2.00	1.68±0.47	0.63±0.10	0.79	0.75	17
12	P16—1 h	PBM, 1.25 h	Slow	No	3.08±1.60	1.56±0.44	0.55±0.12	0.79	0.74	17
13	P16—1 h	PBM, 1.50 h	Slow	No	2.95±1.68	1.66±0.52	0.53±0.13	0.70	0.68	17
14	P16—2 min	PBM, 1.25 h	Slow	No	4.06±1.62	1.50±0.37	0.62±0.11	0.81	0.83	18
15	P16—2 min	PBM, 1.5 h	Slow	No	3.49±1.41	1.46±0.34	0.64±0.08	0.83	0.85	18
16	P16—2 min	PBM, 1.5 h (I)	Slow	No	3.47±1.72	1.57±0.40	0.58±0.08	0.72	0.80	This work
17	P16—1 h	RBM, 20 h	Fast	No	4.22±2.80	1.83±1.03	0.66±0.14	0.84	0.49	This work
18	P16—1 h	RBM, 9 h	Slow	No	6.08±2.38	1.55±0.38	0.59±0.11	0.62	0.83	This work
19	N16—1 h	RBM, 9 h	Slow	No	6.56±2.60	1.55±0.39	0.46±0.10	0.60	0.81	This work

remained constant in these magnets annealed for different periods of time. In general, SF was reduced with high temperature annealing. Based on this initial evaluation, it is proposed that the microstructure and SF can be correlated by

$$sf = 1 - \left[ \frac{\sigma_{GS}}{\bar{X}_{GS}} \left( \frac{\sigma_E}{\bar{X}_E} + \frac{\sigma_R}{\bar{X}_R} \right) \right]. \quad (2)$$

Comparing the squareness factors obtained from Eqs. (1) and (2), samples annealed between 2 and 35 h exhibited a quite satisfactory agreement, with deviations of less than 4%. Equations (1) and (2) were also compared for  $Pr_{16}Fe_{76}B_8$  and  $Nd_{16}Fe_{76}B_8$  sintered magnets prepared with distinct milling times and processing techniques. Roller ball milling (RBM), which is a low-energy milling technique (samples 4–6 for Pr-based compound and samples 7 and 8 for Nd-based compound), was used first. High-energy milling was then carried out in a planetary ball mill (PBM) (samples 9–13 only for the Pr-based compound). The hydrogen decrepitation (HD) stage time was kept constant at 1 h. As expected, the mean grain size of the RBM magnets diminished with increasing milling

time (except for Nd sample 8, probably due to welding of particles during prolonged milling). Mean grain elongation and roundness remained mostly unchanged. The standard deviations showed a tendency for reduction of all the microstructural parameters, indicating the improvement of both size and shape homogeneities, in agreement with the gradual enhancing of SF using Eq. (1) with increasing milling time. The squareness factors obtained based on microstructural parameters and from the demagnetization curve of these magnets showed a satisfactory congruence. The PBM magnets showed a similar behavior in terms of their microstructural homogenization and equivalence of squareness factors. The same behavior was valid even when the HD stage time was reduced from 1 h to 2 min (samples 14 and 15) and also for an isotropic magnet (sample 16). The degree of crystallographic alignment ( $\cos(\Theta)$ ) of the magnets presented in this work is variable due to the distinct processing conditions used. Taking four samples as example, 16, 9, 12, and 15 with  $\langle \cos \Theta \rangle$  equal to 0.51, 0.71, 0.84, and 0.88, respectively, a tendency of better squareness factors for magnets with higher

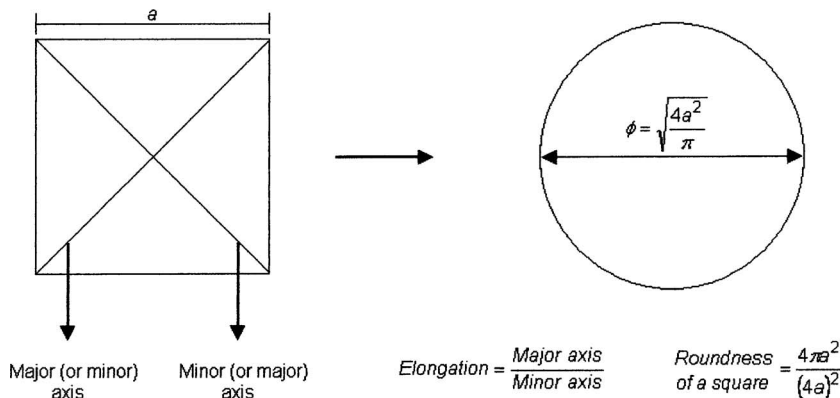


FIG. 1. A square geometric figure transformed into a spherical object, both presenting the same area. Major and minor axes are shown.

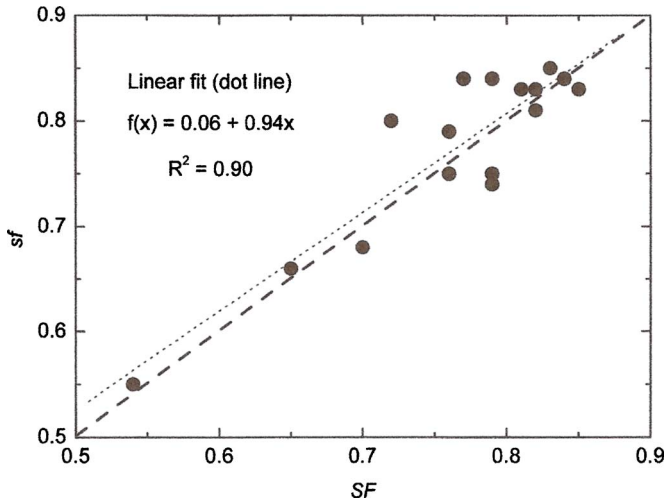


FIG. 2. (Color online) Comparison of the squareness factors obtained using the demagnetization curves and microstructural parameters.

$\langle \cos \Theta \rangle$  can be verified.<sup>7,18</sup> Therefore, possible effects of the texture on the squareness factor are computed in Eq. (2). A previous work has found such a tendency for SmCo magnets, although no relation has been identified.<sup>19</sup> Figure 2 compares the squareness factors obtained using Eqs. (1) and (2). The linear regression, the expression found, and the correlation coefficient are also presented for the purpose of comparison.

Some disparities were also found between these two methods for determining the squareness factors. The *sf* of sample 17 using Eq. (2) showed a 42% lower value than that employing Eq. (1). Possible reasons for this discrepancy are (i) the existence of defects in the interface of Pr<sub>2</sub>Fe<sub>14</sub>B-fcc phases (praseodymium or Pr-rich oxide located at the grain boundaries), which are eliminated with postsintering annealing,<sup>20,21</sup> and/or (ii) an incoherent matching between the crystal lattices of these phases, corrected by heat treatment.<sup>22</sup> It is worth pointing out that the slow cooling used in the present work has the same effect of a stepwise annealing<sup>23</sup> or even a heat treatment at 630 °C for 1 h.<sup>24</sup>

Samples 18 and 19, both milled for 9 h, showed squareness factors differing by more than 20%. This may be related with the volumetric distribution of the (Pr,Nd)<sub>1+ $\epsilon$</sub> Fe<sub>4</sub>B<sub>4</sub> ( $\eta$ ) phase. Low milling times using RBM yield microstructures with large volumes of  $\eta$  at grain boundaries. Reverse domain nucleation begins at the edges of Nd<sub>2</sub>Fe<sub>14</sub>B grains.<sup>25</sup> Therefore, the number of R<sub>2</sub>Fe<sub>14</sub>B grains in contact with the  $\eta$  phase, as well as the contact area, influences the  $M \times H$  curve profile and, consequently, the SF. Equation (2) does not take into account this effect due to the etched surfaces, which explains the differences found. Moreover, these microstructural features are only observable by transmission electron microscopy. Further studies must be carried out to evaluate the effects of secondary phases and alloying elements on Eq. (2). Important features and implicit assumptions that led to the formulation of Eq. (2) must be clarified:

- The expression is dimensionless, in agreement with Eq. (1). This is physically plausible and explains why the mean grain size, the roundness, or the elongation

alone cannot be used to describe the homogeneity of a microstructure.

- Smaller ratios ( $\sigma/\bar{X}$ ) approximate the SF to unity. The size and shape homogeneity of a microstructure must be considered in analyzing the ratios ( $\sigma/\bar{X}$ ), but these parameters must be analyzed jointly.
- The  $\sigma_{GS}$  parameter cannot have a null value because this makes SF=1 and all grains would present exactly the same size, which is experimentally improbable; shape homogeneity would be dispensable, which is incorrect.
- Grain size homogeneity plays a more important role in the SF than does grain shape homogeneity.

#### IV. CONCLUSIONS

A quantitative correlation between the SF and microstructure of R<sub>16</sub>Fe<sub>76</sub>B<sub>8</sub> sintered magnets was proposed. The expression uses grain size, grain elongation, and grain roundness, as well as their respective standard deviations, and is independent of the sample's measured magnetic properties. A fairly good agreement was found in a comparison of the SF obtained by the microstructural method and that calculated from the demagnetization curve for magnets with only three phases and properly processed (considered close to ideal magnets). The SF was improved in magnets with a microstructure of rounder grains and a sharp size distribution. Grain size homogeneity plays a more important role in the SF than does grain shape homogeneity. Appropriate annealing improves shape homogeneity at the expense of size homogeneity. On the other hand, increasing the milling time improves size homogeneity and SF, albeit with a minor influence on shape homogeneity. Therefore, the combination of both appropriate milling and annealing makes it possible to develop a microstructure with a high SF. In nonideal magnets, the disparities found were attributed to defects in the interfacial Pr<sub>2</sub>Fe<sub>14</sub>B-fcc phases at grain boundaries and/or incoherent matching between the crystal lattices of these phases. The presence of secondary phases and their volumetric distribution may also cause discrepancies between the squareness factors of RBM magnets prepared from the magnetic alloy milled for a short period of time (9 h).

#### ACKNOWLEDGMENTS

The authors thank IPEN-CNEN for the use of its facilities and FAPESP for its financial support of this investigation and for the provision of a research grant (E. A. Périgo, Contract No. 2005/04711-2). We are also indebted to L. F. C. P. de Lima for his helpful discussions and to E. Galego and A. G. Fusco for the SEM images.

<sup>1</sup>X. Zhang, Ph.D. thesis, University of Birmingham, 1991.

<sup>2</sup>D. J. Branagan, M. J. Kramer, Y. L. Tang, and R. W. McCallum, J. Appl. Phys. **85**, 5923 (1999).

<sup>3</sup>P. Nothnagel, K.-H. Müller, D. Eckert, and A. Handstein, J. Magn. Mater. **101**, 379 (1991).

<sup>4</sup>S. Szymura, J. J. Wysocki, Yu. M. Rabinovich, and H. Bala, Phys. Status Solidi A **141**, 435 (1994).

<sup>5</sup>K. Uestuener, M. Katter, and W. Rodewald, IEEE Trans. Magn. **42**, 2897 (2006).

- <sup>6</sup>D. W. Scott, B. M. Ma, Y. L. Liang, and C. O. Bounds, *J. Appl. Phys.* **79**, 5501 (1996).
- <sup>7</sup>C. N. Christodoulou, J. Schlup, and G. C. Hadjipanayis, *J. Appl. Phys.* **61**, 3760 (1987).
- <sup>8</sup>A. Handstein, J. Schneider, K.-H. Müller, R. Krewenka, R. Grössinger, and H. R. Kirchmayr, *J. Magn. Magn. Mater.* **83**, 199 (1990).
- <sup>9</sup>W. Rodewald, B. Wall, and W. Fernengel, *IEEE Trans. Magn.* **33**, 3841 (1997).
- <sup>10</sup>A. Binner, J. Schneider, and C. Stiller, *J. Magn. Magn. Mater.* **101**, 427 (1991).
- <sup>11</sup>J. F. Herbst, *Rev. Mod. Phys.* **63**, 819 (1991).
- <sup>12</sup>Y. Tsubokawa, R. Shimizu, S. Hirosawa, and M. Sagawa, *J. Appl. Phys.* **63**, 3319 (1988).
- <sup>13</sup>R. Ramesh, G. Thomas, and B. M. Ma, *J. Appl. Phys.* **64**, 6416 (1988).
- <sup>14</sup>T. Shimoda, I. Okonogi, and K. Teraishi, *Proceedings of the Fifth International Workshop on Rare-Earth Cobalt Permanent Magnets and Their Applications* (University of Dayton, Dayton, OH, 1981) p. 597.
- <sup>15</sup>*ASM Handbook—Powder Metal Technologies and Applications*, edited by P. W. Lee (American Society for Metals, Metals Park, OH, 1998), Vol. 7, p. 585.
- <sup>16</sup>G. A. Baxes, *Digital Image Processing: Principles and Applications* (Wiley, New York, 1994).
- <sup>17</sup>E. A. Périco, E. P. Soares, R. M. L. Neto, C. C. Motta, and R. N. Faria, *Mater. Res.* **10**(3), 313 (2007).
- <sup>18</sup>E. A. Périco, N. B. Lima, H. Takiishi, C. C. Motta, and R. N. Faria, *J. Magn. Magn. Mater.* (unpublished).
- <sup>19</sup>D. L. Martin, H. F. Mildrum, and S. R. Trout, *Proceedings of the Eighth International Workshop on Rare Earth Permanent Magnets and Their Applications* (University of Dayton, Dayton, OH, 1985), p. 269.
- <sup>20</sup>A. G. Popov, T. Z. Puzanova, V. S. Gaviko, D. Yu. Vasilenko, and V. P. Vyatkin, *Phys. Met. Metallogr.* **101**, 544 (2006).
- <sup>21</sup>F. Vial, F. Joly, E. Nevalainen, M. Sagawa, K. Hiraga, and K. T. Park, *J. Magn. Magn. Mater.* **242–245**, 1329 (2002).
- <sup>22</sup>K. Makita and O. Yamashita, *Appl. Phys. Lett.* **74**, 2057 (1999).
- <sup>23</sup>J. Ormerod, *J. Less-Common Met.* **111**, 49 (1985).
- <sup>24</sup>P. J. McGuinness, Ph.D. thesis, University of Birmingham, 1989.
- <sup>25</sup>J. Pastushenkov, K. D. Durst, and H. Kronmüller, *Phys. Status Solidi A* **104**, 491 (1987).